ARTICLE

Copper(II) and Zinc(II) Complexes of Mono- and Bis-1,2,3-triazole-substituted Heterocyclic Ligands

Received 00th January 20xx,
Accepted 00th January 20xx

DOI: 10.1039/x0xx00000x

Natalija Pantalon Juraj,[a] Marko Krklec,[a,b] Tiana Novosel,[a,b] Berislav Perić,[a] Robert Vianello,[*,a] Silvana Raić-Malić[*,b] and Srećko I. Kirin[*,a]

Chelating 1,4-disubstituted mono- (**8a**–**8d**) and bis-1,2,3-triazole-based (**9a**–**11a**) ligands were prepared by regioselective copper(I)-catalysed 1,3-dipolar cycloaddition of terminal alkynes with aromatic azides, together with bioconjugate **13a** synthesized by amide coupling of L-phenylalanine methyl ester to **11a**. Cu(II) and Zn(II) complexes were prepared and single crystal structures were determined for complexes $\mathbf{8a_{Cu}}$, $\mathbf{8d_{Cu}}$, $\mathbf{9c_{Cu}}$ and $\mathbf{10c_{Cu}}$, as well as the free ligands **10a** and **10c**. The *in situ* prepared Zn(II) complexes were studied by NMR spectroscopy, while the stoichiometry of the Cu(II) complexes in solution was determined by UV-Vis titrations and confirmed by the electronic structure DFT calculations at the (SMD)/M05-2X/6-31+G(d)/LanL2DZ + ECP level of theory.

Introduction

The function of the 1,2,3-triazolyl moiety, derived from copper(I)-catalysed azide–alkyne cycloaddition (CuAAC), has recently been expanded to coordination chemistry of transition metals.[1–6] Regioselective formation of 1,4-disubstituted 1,2,3-triazole-based mono-, bi- or multidentate chelating ligands has received considerable attention because of its broad application in drug development, optics, redox sensing, fluorescence and catalysis.[2,3,7–13] The large dipole moment of triazoles, around 5 D, allows easy formation of hydrogen bonds, as well as dipole-dipole and π-interactions, which can favour their binding to biological targets and improve their solubility.[14] Moreover, 1,2,3-triazoles are found to be versatile ligands that can coordinate to metals through the N3, N2 and C5 donor sites, with preferential coordination at the N3 atom.[12,15] *N*-coordination modes offer complexation via anionic and cationic nitrogen donors of triazolate and triazolium ions, respectively, while CH-deprotonation of the triazole and the triazolium affords carbanionic and mesoionic carbene donors available for metal coordination.[16]

In hexacoordinated $\mathbf{ML_2}$ complexes of tridentate ligands, depending on the angles between the donor atoms of the ligand, different geometrical isomers are possible; *mer*, *trans-fac* and Δ- or λ- *cis-fac*.[17] In our previous research, similar tridentate ligand systems and their stereochemical preferences were described. While iminodiacetamide (**imda**) ligands showed preference towards forming $\mathbf{ML_2}$ complexes that are *trans-fac* isomers,[18–20] bis(2-picolyl)amine (**bpa**) ligands showed versatile coordination possibilities,[17,21] making it less straightforward to obtain complexes of $\mathbf{ML_2}$ stoichiometry. However, when **bpa** ligands form $\mathbf{ML_2}$ complexes, they are preferentially *cis-fac* isomers.[3,22]

In this work, we present the synthesis of Cu(II) and Zn(II) complexes of $\mathbf{ML_2}$ stoichiometry with bis-1,2,3-triazole and mono-1,2,3-triazole-2,2′-dipyridylamine ligands, and evaluate different effects determining the stoichiometry, geometry and stereochemistry of the prepared complexes. In addition, derivatives containing a methyl ester protecting group offer the possibility of easy conjugation to a wide range of biomolecules, such as amino acids. Our aim was to study the stereochemical preference of the bis-1,2,3-triazole ligand system. In literature, there are only few transition metal complexes involving such ligands, and their stereochemical preference has not been studied so far. In the CSD database search of transition metal complexes with bis-1,2,3-triazole ligands, seventeen **ML** and ten $\mathbf{ML_2}$ complexes are found. All reported $\mathbf{ML_2}$ complexes[23–25] are *trans-fac* isomers and have weakly coordinating anions, while the majority of **ML** complexes are found with strongly coordinating anions, such as thiocyanate,[26,27] halogenides[27,28] or azides,[29,30] where the anion occupies the remaining coordination sites of the metal.

[a] *Ruđer Bošković Institute, Zagreb, Croatia.*
[b] *Faculty of Chemical Engineering and Technology, University of Zagreb, Zagreb, Croatia.*

† Footnotes relating to the title and/or authors should appear here.
Electronic Supplementary Information (ESI) available: [details of any supplementary information available should be included here].

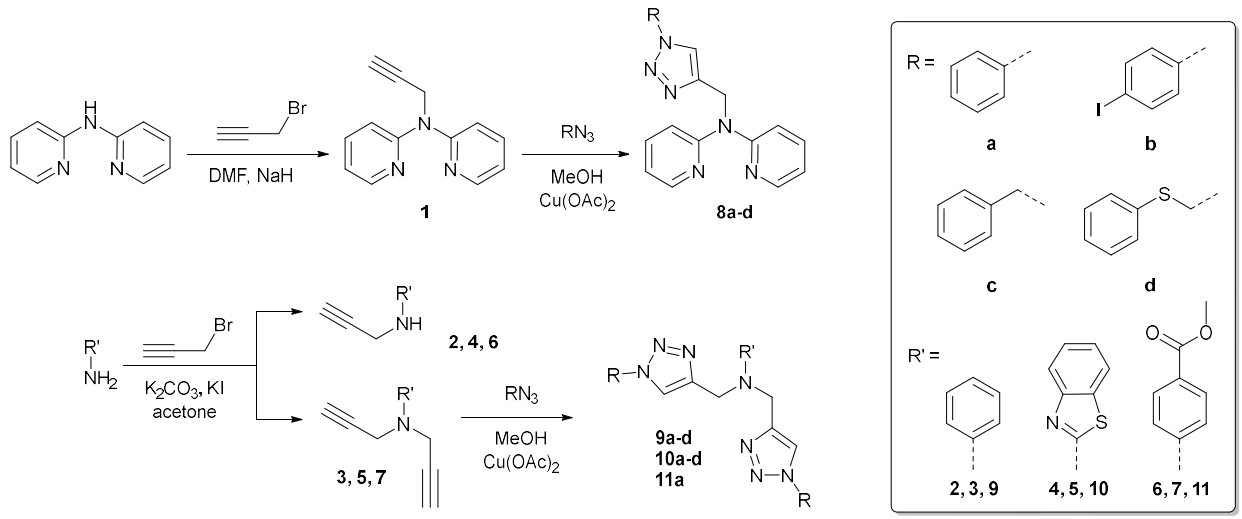

Scheme 1. Synthesis of alkynes **1**–**7**, mono-1,2,3-triazoles **8a**–**8d** and bis-1,2,3-triazoles **9a**–**11a**.

Results and discussion

Ligands, synthesis and solid-state characterization.[31,32] Mono-1,2,3-triazole derivatives (**8a**–**8d**) were prepared in two steps. Starting with propargylation of 2,2′-dipyridylamine, mono-alkyne **1** was obtained and subsequently reacted with a series of azides: azidobenzene (a), 1-azido-4-iodobenzene (b), benzyl azide (c) and azidomethyl phenyl sulfide (d) in a regioselective copper(I) catalysed Huisgen cycloaddition reaction, forming 1,4-disubstituted mono-1,2,3-triazoles **8a**–**8d** (Scheme 1). The copper(II) salt, $Cu(OAc)_2$, was used for *in situ* generation of Cu(I).[33,34]

A similar two-step procedure was used to prepare bis-1,2,3-triazoles **9a**–**11a**. Alkynes **2**–**7** were prepared by propargylation of aniline (**2**, **3**)[35], 2-aminobenzothiazole (**4**, **5**)[36] or methyl-4-aminobenzoate (**6**, **7**). In the propargylation reaction, mono- and bis-alkynes were obtained and the bis-alkynes were reacted further with a series of azides (a-d), forming bis-1,2,3-triazoles **9a**–**11a** (Scheme 1).

In order to increase the flexibility and coordination possibilities of ligand **11a**, an attempt was made to introduce an additional CH_2 linker. In particular, a CH_2 group was added between the central amine nitrogen and the phenyl group; methyl-4-(aminomethyl)benzoate was used instead of methyl-4-aminobenzoate (Figure S6). However, the propargylation reaction gave significantly lower yields than with the aromatic methyl-4-aminobenzoate. A similar synthesis of *N,N*-di-2-propynyl-benzenemethanamine was reported with a low yield.[37] The amino acid bioconjugate **13a** was prepared from ligand **11a** in a two-step procedure (Scheme 2). The methyl ester protecting group was removed by hydrolysis in alkaline conditions[38] and the carboxylic acid **12a** was used in a standard amide coupling reaction to obtain the ligand **13a**.

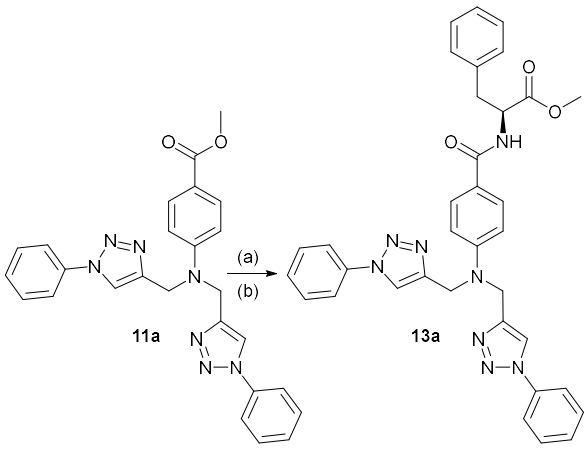

Scheme 2. Synthesis of ligand **13a**. (a) CH_2Cl_2/CH_3OH (9:1), 1 M NaOH; (b) TBTU, HOBt, DIPEA, H-Phe-OMe × HCl.

The prepared ligands **8a**–**13a** were purified using column chromatography, and characterised by ^1H, ^{13}C NMR and IR spectroscopy and mass spectrometry. Single crystals suitable for X-ray diffraction were obtained for ligands **10a** and **10c** (Figure 1). Ligand **10a** crystallizes in the *Pbca* space group, with 8 molecules in the unit cell, while ligand **10c** crystallizes in the $I4_1/a$ space group, with 16 molecules in the unit cell. Ligand **10a** has a bent conformation, where the distance between centroids of the triazole rings is 3.509 Å. In the crystal structure of ligand **10c**, the distance between centroids of the triazole rings is 6.440 Å and the conformation can be described as stretched.

Copper(II) complexes, synthesis and solid-state characterization. Cu(II) complexes were prepared by mixing boiling methanol solutions of $Cu(BF_4)_2$ x nH_2O with boiling methanol or dichloromethane solutions of the ligand, in a 2:1 ligand to metal ion ratio. The complexes were crystallized by method of slow evaporation or vapour diffusion of diethyl-ether.

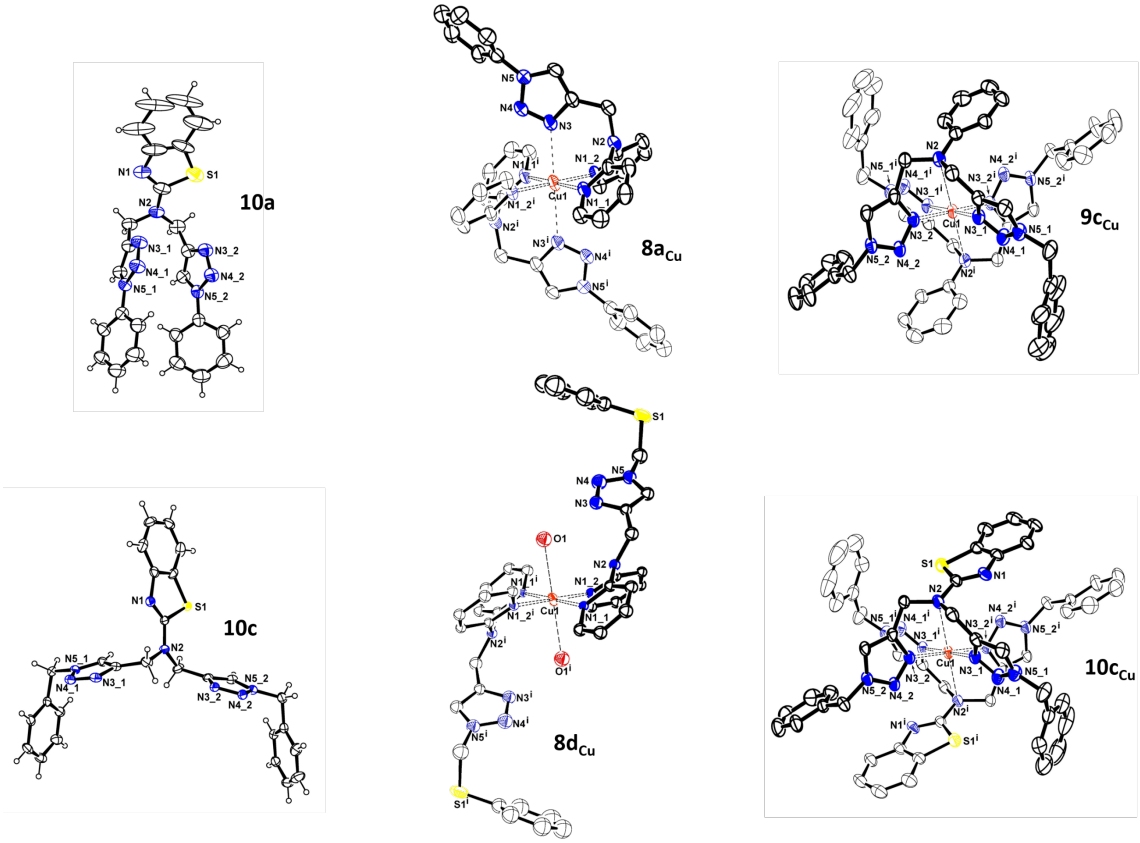

Figure 1. Ortep-III diagrams for structures of ligands **10a** and **10c** and **ML$_2$** complexes **8a$_{Cu}$**, **8d$_{Cu}$**, **9c$_{Cu}$** and **10c$_{Cu}$** with ellipsoids of 30% probability level and labelled heteroatoms. For **10c**, only the higher occupied positions of S1 and N1 atoms are shown. The disorder is shown in Figure S9. Hydrogen atoms are omitted for clarity and for **8c$_{Cu}$** only the higher occupied position of one disordered phenyl ring is shown. The anions (BF_4^- in **8a$_{Cu}$**, and SiF_6^{2-} in **8d$_{Cu}$**, **9c$_{Cu}$** and **10c$_{Cu}$**) are omitted for clarity, complete Ortep-III diagrams are given in ESI. In order to emphasize the position of ligands in the complexes, one ligand is shown bold and other one, which is related by centre of symmetry in the Cu atom, is shown light. [Symmetry code (i): 1-*x*, 1-*y*, 1-*z*].

Single crystals suitable for X-ray diffraction were obtained for metal complexes **8a$_{Cu}$**, **8d$_{Cu}$**, **9c$_{Cu}$** and **10c$_{Cu}$** (Figure 1). Selected bond lengths and angles are shown in Tables S3 and S4. All four metal complexes have **ML$_2$** stoichiometry in the solid state. The weakly coordinating BF_4^- anion was used in synthesis to avoid interaction of the anion with the metal center.[39] As found in literature[40,41], and in our previous publications[18,21], the BF_4^- anion can undergo decomposition, forming fluoride anions. These F^- ions can further react with the glass reaction vessel forming SiF_6^{2-} anions, that were found in the crystal structures of **8d$_{Cu}$**, **9c$_{Cu}$** and **10c$_{Cu}$**. Presence of the larger SiF_6^{2-} anion likely facilitates crystallization due to the large size of the cation.[42,43]

In complexes **8a$_{Cu}$** and **8d$_{Cu}$**, the two ligands are coordinated via nitrogen atoms from the 2,2′-dipyridylamine groups forming equatorial planes of the **[CuN$_6$]** or **[CuN$_4$O$_2$]** coordination octahedra, respectively (Figure 1). In **8a$_{Cu}$**, the N3 triazole nitrogen atoms of both ligands are coordinated in the apical positions, while for **8d$_{Cu}$** the triazole groups are not coordinated to the metal and the apical positions are occupied by water molecules present in the solution due to the hygroscopic nature of $Cu(BF_4)_2$. For **8d$_{Cu}$**, the poor quality of the data recorded at ϑ angles higher than 35°, resulted in poor data to parameter ratio, thus the precision of geometry parameters for this structure is lower than for other structures presented in this work. However, the structure of **8d$_{Cu}$** was taken for comparison with **8a$_{Cu}$**, to show different binding modes of mono-triazole ligands. The complex cations of **8a$_{Cu}$** and **8d$_{Cu}$** are C_i symmetric and crystallize in the *P*-1 space group. Geometry parameters of the **[CuN$_6$]** or **[CuN$_4$O$_2$]** coordination octahedra are given in Table S3.

A CSD search of first row transition metal **ML$_2$** complexes of 2,2′-dipyridylamine-CH_2-R ligands showed that all seven reported complexes are hexacoordinated and have regular octahedral geometries as determined by the program FindGeo.[44] In all the literature complexes, two 2,2′-dipyridylamine ligands occupy four coordination sites, while the remaining two coordination sites are occupied by anion or solvent molecules. The complexes are *trans* isomers in regard to the coordinated anion/solvent,[45,46] with the exception of one Ni(II) complex with *cis* coordination of DMF solvent molecules.[47]

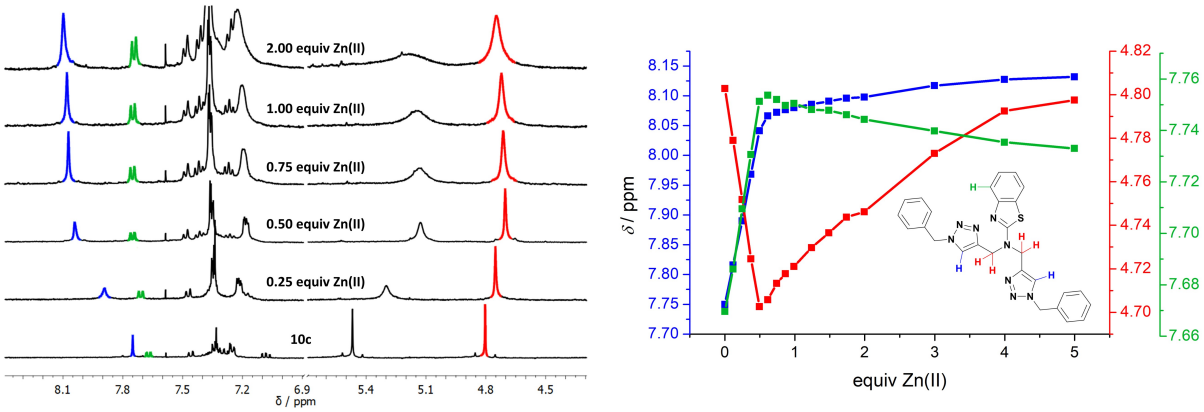

Figure 2. ^{1}H NMR (CD_3CN) titration of ligand **10c** with $Zn(CF_3SO_3)_2$ (left) and chemical shifts of selected protons (right).

Complexes of bis-triazole ligands, $\mathbf{9c_{Cu}}$ and $\mathbf{10c_{Cu}}$ (Figure 1) are mutually similar in structure, crystallizing in the $P2_1/c$ space group, with two molecules of C_i symmetry in the unit cell. Octahedral geometry with an elongated z-axis is common for Cu(II) complexes with the unpaired electron in the $d_{x^2-y^2}$ orbital.[48] The N3_1 and N3_2 triazole nitrogen atoms of the two ligands are coordinated in the equatorial planes of $\mathbf{9c_{Cu}}$ and $\mathbf{10c_{Cu}}$. However, the Cu-N2 distances, where N2 is the central amine nitrogen atom, in complexes $\mathbf{9c_{Cu}}$ and $\mathbf{10c_{Cu}}$ are longer than expected for Jahn-Teller distortion; 2.782 Å and 2.894 Å in $\mathbf{9c_{Cu}}$ in $\mathbf{10c_{Cu}}$, respectively (Table S3). Currently there are no published Cu(II) complexes with bis-triazole ligands of $\mathbf{ML_2}$ stoichiometry to allow for a comparison of bond lengths. In a CSD search of $\mathbf{CuL_2}$ complexes with tridentate nitrogen donor ligands forming 5-membered chelate rings (Table S2), complexes of bis(2-pyridylmethyl)amine (**bpa**) and diethylenetriamine ligands were found. Five of the complexes have compressed octahedral geometry, and ten have elongated octahedral, with most axial bonds around 2.4 Å, and the longest axial bond was 2.607 Å, still significantly shorter than in $\mathbf{9c_{Cu}}$ and $\mathbf{10c_{Cu}}$. Average values for Cu-N(triazole) and Cu-N(amine) bond lengths are found to be 2.048 Å and 2.140 Å respectively, calculated as an average for the eleven Cu(II) complexes of ligands containing a bis-triazole moiety found in the CSD database.[29,49–51] For complexes $\mathbf{9c_{Cu}}$ and $\mathbf{10c_{Cu}}$, due to the elongated Cu-N2 distance, the complexes can be described as pseudo *trans-fac* isomers, with N2-M-N2 angles 180° and N3_1-M-N3_2 angles 93.45 and 92.35° for $\mathbf{9c_{Cu}}$ and $\mathbf{10c_{Cu}}$, respectively (Table S4).

The IR (KBr) spectra of the Cu(II) complexes showed a shift of the triazole C-H band, for example from 3116 cm^{-1} in **9c** to 3148 cm^{-1} in $\mathbf{9c_{Cu}}$ and from 3119 cm^{-1} in **10c** to 3140 cm^{-1} $\mathbf{10c_{Cu}}$ upon coordination to Cu.

Characterization in solution. The metal complexes were studied in solution by NMR and UV-Vis spectroscopy. For the NMR measurements, Zn(II) salts were used due to the paramagnetic nature of Cu(II). Zn(II) complexes were prepared *in situ*, by dissolving a mixture of the ligand and Zn(II) salt in deuterated solvent. The stoichiometry, anion, solvent and temperature were varied. Upon complexation, a shift of NMR signals is observed, most notably for the triazole NH and CH_2 protons (Tables S5-S8).

To study the equilibrium in solution, an NMR titration was performed for ligand **10c**, by adding increasing equivalents of Zn(II) (Figure 2, full titration spectra are given in Figure S18). At each titration point, only a single set of signals was observed, indicating exchange processes faster than the NMR measurement timescale.[52] The largest changes were observed between 0 and 0.5 equiv of added Zn(II), indicating the formation of $\mathbf{ML_2}$ complexes. The triazole and benzothiazole protons showed a downfield shift, while the α-CH_2 protons showed an upfield shift. At higher equivalents of Zn(II), the benzothiazole protons shifted upfield, while triazole and α-CH_2 protons shifted downfield. However, the shifts became smaller for added equivalents higher than 0.5, indicating formation of **ML** complexes. The stability constants were too large to be accurately determined from these experiments.[53]

Since the spectra show species in fast exchange, spectra of isolated **ML** or $\mathbf{ML_2}$ complexes could not be defined. In Figures S19-S21, spectra of the free ligands compared to *in situ* prepared complexes in a 2 L : 1 Zn(II) ratio, that would roughly correspond to the $\mathbf{ML_2}$ species are shown. The large shifts of the mono-triazole protons ($\Delta\delta$ = 0.2-0.5 ppm) are an indication that the triazole group is coordinated in all the Zn(II) complexes with mono-triazole ligands, since the non-coordinated triazole group would be far away from the metal and no significant shift would be expected.

In hexacoordinated $\mathbf{ML_2}$ complexes of tridentate ligands with an α-CH_2 group, geminal splitting of the α-CH_2 protons can be indicative of the type of geometrical isomer in solution. In *trans-fac* isomers, that would correspond to the Cu(II) crystal structures, the α-CH_2 protons are expected to show two doublets of geminal coupling.[18] However, the spectra of Zn(II) complexes with ligands **9a**–**10d** showed a single α-CH_2 peak (Figures S20-S21). If a long Zn-N2 distance is assumed (see Computational analysis of zinc complexes), nitrogen inversion would be possible and the α-CH_2 protons equivalent, showing a single sharp peak.[18] Furthermore, fast ligand exchange could also cause the equivalence of α-CH_2 protons.

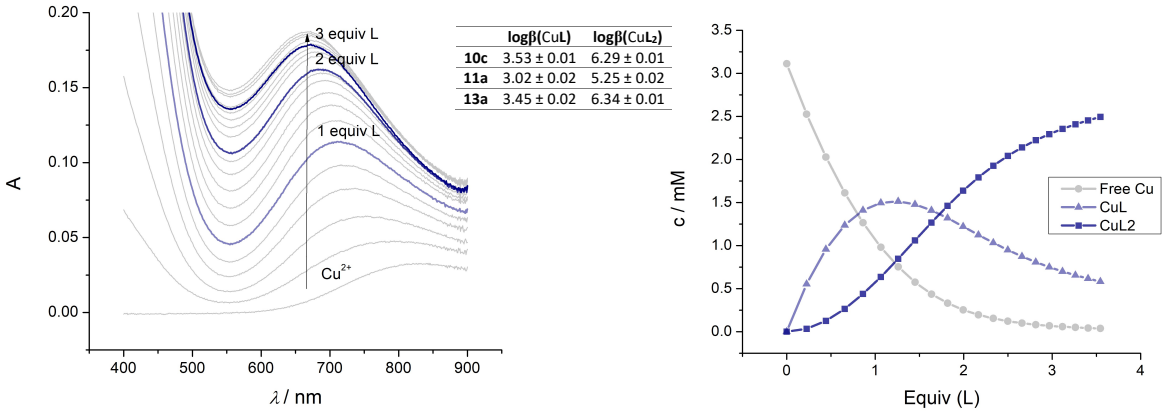

	logβ(CuL)	logβ(CuL₂)
10c	3.53 ± 0.01	6.29 ± 0.01
11a	3.02 ± 0.02	5.25 ± 0.02
13a	3.45 ± 0.02	6.34 ± 0.01

Figure 3. UV-Vis titration of Cu(II) with ligand **13a** (left) and species distribution (right) in a 1:1 CH_3OH:CH_2Cl_2 solvent mixture.

Splitting of the α-CH_2 peak was observed for [Zn(**13a**)$_2$]$(CF_3SO_3)_2$, as the chirality of the ligand lowers the symmetry of the complex (Figure S28).

An attempt was made to study a stronger Zn-N2 bond and/or slower ligand exchange at lower temperature (−40°C). For complexes [Zn(**9a**)$_2$]$(BF_4)_2$ and [Zn(**10a**)$_2$]$(BF_4)_2$, no significant changes were observed, while for [Zn(**9a**)(CD_3CN)]$(BF_4)_2$, [Zn(**9c**)$_2$]$(BF_4)_2$, [Zn(**10c**)$_2$]$(BF_4)_2$ and [Zn(**10d**)$_2$]$(BF_4)_2$, peak broadening was observed, indicating slower ligand exchange, becoming intermediate compared to the NMR timescale (Figure S22). Temperatures lower than −40°C were not possible due the melting point of CD_3CN (−45°C).

The formation of complexes of different stoichiometry can be influenced by the coordinating ability of the counterion.[21] To study the influence of the counterion, complexes of ligands **9c** and **10c** were prepared with Zn(II) salts of three counterions; BF_4^-, NO_3^-, Br^-; ranging from weak to strong coordinating ability.[39] When comparing spectra of complexes with all three anions at a 2 L to 1 Zn(II) ratio, most peaks have similar shifts, however, different shifts of the triazole protons are observed (Figures S23 and S24), indicating either influence on the equilibrium where the different shift is caused by a different ratio of **ML** and **ML$_2$** complexes in fast exchange, and/or the difference is caused due to the different electronic effects of anions coordinated to the remaining three coordination sites of Zn(II) in the **ML** complexes. At a 1 L to 6 Zn(II) ratio, peaks are shifted compared to the 2 L to 1 Zn(II) ratio, indicating a different equilibrium at different ratios (Figure S25).

The Zn(II) complex of ester **11a** shows signal broadening compared to the free ligand. For bioconjugate **13a**, complexes with $Zn(BF_4)_2$ and $Zn(CF_3SO_3)_2$ at a 2 L to 1 Zn(II) ratio were similar, regardless of the anion. With **13a** and $Zn(CF_3SO_3)_2$ at different ratios, a large shift of triazole protons was observed for the 2:1 ratio compared to the free ligand (0.43 ppm), while for the 1:1 ratio compared to 2:1, the shift is much smaller (0.03 ppm). This is similar to the NMR titration of **10c**, where the shift of the triazole peak for 2:1 compared to the free ligand was 0.29 ppm and for 1:1 compared to 2:1, the shift was 0.04 ppm.

The Cu(II) complexes were characterized by UV-Vis spectroscopy (Figures S30-S38). For ligands **10c**, **11a** and **13a**, UV-Vis titrations were performed by adding the ligand in the solution of Cu(II) to a solution of Cu(II) of the same concentration to avoid dilution.[53] A 1:1 CH_3OH:CH_2Cl_2 solvent mixture was used, due to low solubility of the ligands in polar solvents and the metal salt in non-polar solvents. $Cu(CF_3SO_3)_2$ was used due to the hygroscopic nature of $Cu(BF_4)_2$ used in the synthesis of complexes. Binding constants were determined for **ML** and **ML$_2$** complexes using the HypSpec2014 software[54] and their values are similar for complexes of all three ligands in the given conditions (Figure 3) and indicate somewhat greater stability of **ML** complexes. Furthermore, the calculated species distributions (Figures S32, S35, S38) show that a mixture of **ML** and **ML$_2$** complexes is present even at 3 equiv of added ligand. Here it should be noted that the $CF_3SO_3^-$ anion used in titrations has a slightly stronger coordinating ability[39] than the BF_4^- anion used in the synthesis of complexes, which could cause greater stability of the **ML** complexes due to possible coordination of the $CF_3SO_3^-$ anion to the copper ion.

CD spectra were recorded for the addition of chiral ligand **13a** to a Cu(II) solution. The spectra at different added equivalents show maxima of low intensity around 650 nm, indicating only weak transfer of chirality from the chiral ligand to the copper ion (Figure S39). This weak chirality transfer is expected due to the large distance of the chiral moieties and the rather rigid side chains, preventing the formation of hydrogen bonded secondary structures.[55]

Computational analysis. DFT calculations at the (SMD)/M05-2X/6-31+G(d)/LanL2DZ + ECP level of theory were performed for mono- and bis-triazole complexes of **[ML$_2$]$^{2+}$** stoichiometry. Since the anions (BF_4^- or SiF_6^{2-}) do not coordinate to the metal, only the complex cations were calculated; the anions were not considered due to simplicity.[18,21]

Mono-triazole ligands **8a**–**8d** can act both as bidentate ligands, by coordinating only with the dipyridyl group as found in **8d$_{Cu}$**, or as tridentate ligands, by including the triazole group in

the coordination, as in **8a$_{Cu}$**. The corresponding complexes **[Cu(14a)$_2$]$^{2+}$** and **[Cu(14b)$_2$]$^{2+}$** (Figure 4) were calculated and the structures with coordinated or non-coordinated triazole group optimized to determine the reason for different coordination modes observed in complexes **8a$_{Cu}$** and **8d$_{Cu}$**. In the later set of systems, the remaining coordination positions around the metal cation were occupied by two water molecules. However, we observed no clear electronic or structural effect to which we could attribute the mentioned coordination differences among ligands. Still, if one considers the ligand fragments shown on Figure 4, the atomic charge on potentially coordinating N-3 in **[Cu(14a)$_2$]$^{2+}$** in acetonitrile is –0.26 |e|, considerably more negative than the remaining two nitrogen atoms in the triazole ring; q(N-1) = +0.18 |e| and q(N-2) = –0.24 |e|. In **[Cu(14b)$_2$]$^{2+}$**, the charge on the analogous N-3 is reduced by 15% to –0.22 |e|, indicating that the smaller effective charge on the coordinating nitrogen atom is likely responsible for the bidentate coordination observed in **8d$_{Cu}$**. The charges on the remaining two nitrogen atoms in **[Cu(14b)$_2$]$^{2+}$** are q(N-1) = +0.09|e| and q(N-2) = –0.18 |e|.

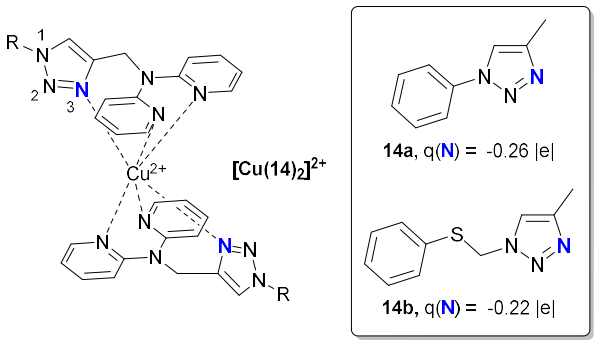

Figure 4. Structures of calculated **ML$_2$** complexes of mono-triazole ligands **14a** and **14b** with Cu(II).

Relative stabilities of Cu(II) and Zn(II) **ML$_2$** complexes with bis-triazole ligands **15a**–**15d** were calculated (Figure 5). Ligands **15a**–**15d** used in calculations have methyl substituents on the triazole rings and methyl, isopropyl, phenyl or benzothiazole groups on the central amine nitrogen. For each complex, relative stabilities of *cis-fac*, *mer* and *trans-fac* isomers were considered, both in the gas phase and acetonitrile solution. In our previous publications,[17,18,21] calculations in acetonitrile consistently offered a much better agreement with the experimental results, so only the results in acetonitrile will be discussed here (Table 1). Selected bond lengths and angles of calculated structures are shown in Tables S10-S12 and the coordination polyhedra were analysed using the program FindGeo.[18,44]

For Zn(II) complexes **[Zn(15)$_2$]$^{2+}$**, smaller alkyl substituents on the central amine nitrogen favour *trans-fac* isomers. Larger aromatic groups introduce steric crowding in these positions among ligands, thus the *N*-phenyl group promotes the *mer* isomer. Interestingly, the *N*-benzothiazole moiety gives the *cis-fac* isomer as the most stable and this is attributed to the favourable π–π stacking interactions between the benzothiazole fragment on one ligand and triazole units on the other.

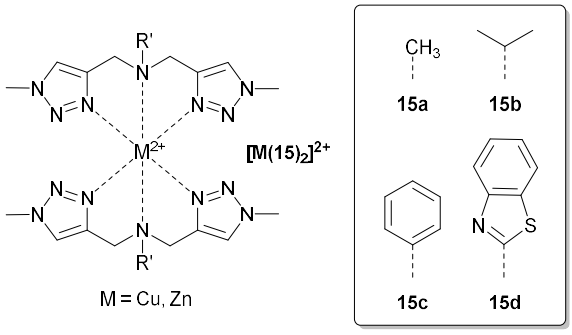

Figure 5. Structures of calculated **ML$_2$** complexes of bis-triazole ligands **15a–15d** with Zn(II) and Cu(II).

The size of the substituent on the amine nitrogen also affects the coordination mode. Specifically, ligands with smaller groups are predominantly tridentate, while when larger groups are introduced, the ligands are mainly bidentate, as the corresponding metal-N(amino) bonds become elongated and ligands coordinate the metal only with the triazole nitrogen atoms. In *mer*-**[Zn(15c)$_2$]$^{2+}$**, the octahedral geometry becomes extended with the N(amino)-Zn distances of 2.679 and 2.891 Å.

Table 1. Relative Gibbs free energies (in kcal mol^{-1}) and distances between the metal and amine nitrogen atom of different structural isomers, involving the Zn(II) or Cu(II) cation and various ligands in the 2 L to 1 M ratio. All values are obtained by the M05-2X/6-31+G(d)/LanL2DZ + ECP model. Acetonitrile solvent effects are modeled through the implicit SMD solvation.

Complex	Isomer	Zn(II)	Cu(II)	N2-Zn-N2^i (Å)	N2-Cu-N2^i (Å)
	cis-fac	2.0	2.3	2.394	2.494
				2.357	2.164
[M(15a)$_2$]$^{2+}$	*mer*	1.7	**0.0**	2.272	**2.116**
				2.289	**2.097**
	trans-fac	**0.0**	3.5	**2.282**	2.405
				2.282	2.406
	cis-fac	5.1	3.8	2.603	2.207
				2.441	2.760
[M(15b)$_2$]$^{2+}$	*mer*	3.1	6.8	2.316	2.436
				2.320	2.437
	trans-fac	**0.0**	**0.0**	**2.425**	**2.621**
				2.425	**2.624**
	cis-fac	0.9	3.1	2.614	2.724
				2.613	2.278
[M(15c)$_2$]$^{2+}$	*mer*	**0.0**	3.5	**2.679**	2.523
				2.891	2.522
	trans-fac	1.9	**0.0**	2.467	**2.670**
				2.465	**2.561**
	cis-fac	**0.0**	2.3	**3.136**	3.059
				3.156	3.188
[M(15d)$_2$]$^{2+}$	*mer*	5.3	6.3	2.876	3.289
				2.876	3.200
	trans-fac	6.7	**0.0**	2.877	**3.066**
				2.570	**3.206**

^{i} symmetry related atom

The same situation is observed for the *cis-fac* isomer, while the ligands are classically tridentate in the *trans-fac* isomer, yet the latter is the least stable among the corresponding isomers. Ligand **15d** is bidentate in all three geometrical isomers of **[Zn(15d)$_2$]$^{2+}$** with the *cis-fac* being the most stable, linked with large N(amino)-Zn distances of 3.136 and 3.156 Å. These results agree with the NMR measurements, showing that large Zn-N2 distances enable nitrogen inversion leading to equivalence of α-CH_2 protons, even at −40°C.

For **ML$_2$** complexes with Cu(II), *trans-fac* isomers are the most stable, with the exception of **[Cu(15a)$_2$]$^{2+}$** involving the smallest methyl group substituent, where *mer* is most favoured. Ligands in **[Cu(15a)$_2$]$^{2+}$**, **[Cu(15b)$_2$]$^{2+}$** and **[Cu(15c)$_2$]$^{2+}$** are predominantly tridentate, while **15d** is mainly bidentate in all three calculated isomers of **[Cu(15d)$_2$]$^{2+}$**. Specifically, in the most stable *trans-fac* isomer, the geometry of **[Cu(15d)$_2$]$^{2+}$** is such that both N(amino)-Cu distances again stretch over 3 Å and are calculated to be 3.066 and 3.206 Å.

Lastly, the calculations clearly reveal that the most stable isomer of complexes **[Cu(15c)$_2$]$^{2+}$** and **[Cu(15d)$_2$]$^{2+}$** is *trans-fac*, which is in excellent agreement with the experimental structures **9c$_{Cu}$** and **10c$_{Cu}$**.

Conclusions

Mono- and bis-1,2,3-triazole ligands, **8a**–**11a** were prepared by Cu(I) catalysed cycloaddition of azides and alkynes. Amino acid bioconjugate **13a** was obtained by standard amide coupling. Crystal structures were determined for two ligands, **10a** and **10c**, and four Cu(II) complexes, **8a$_{Cu}$**, **8d$_{Cu}$**, **9c$_{Cu}$** and **10c$_{Cu}$**. The Cu(II) complexes were characterized in solution by UV-Vis spectroscopy, while NMR spectroscopy was used for characterization of diamagnetic Zn(II) complexes in solution. Stereochemical preferences of different ligands were studied with DFT calculations.

In the crystal structures of **8a$_{Cu}$** and **8d$_{Cu}$** the complexes have **ML$_2$** stoichiometry; ligand **8a** acts as a tridentate ligand, while ligand **8d** is bidentate and the remaining coordination sites are occupied by water molecules. In complexes **9c$_{Cu}$** and **10c$_{Cu}$**, the triazole groups are coordinated to Cu in the equatorial plane, while the Cu-N2 distance is elongated and the complexes can be considered as pseudo *trans-fac* isomers.

The UV-Vis titrations show formation of complexes of **ML** and **ML$_2$** stoichiometry for Cu(II) complexes of ligands **10c**, **11a** and **13a**. NMR spectra of Zn(II) complexes also revealed formation of complexes of **ML** and **ML$_2$** stoichiometry that are in fast exchange compared to the NMR timescale. Equivalence of the α-CH_2 signal indicates nitrogen inversion of the central amine nitrogen, due to the large Zn-N2 distance, observed also in the calculated Zn(II) complexes.

DFT calculations show that larger negative charge on the N3 atom in **[Cu(14a)$_2$]$^{2+}$** compared to **[Cu(14b)$_2$]$^{2+}$** could be the reason for different coordination modes observed in crystal structures of **8a$_{Cu}$** and **8d$_{Cu}$**. Calculations for **ML$_2$** complexes of bis-triazole ligands **15a**–**15d** showed that smaller alkyl groups on the central nitrogen atom favour *trans-fac* isomers in Zn(II) complexes as opposed to Cu(II) complexes, where *trans-fac* isomers are formed predominantly for ligands with larger groups on the central amine nitrogen. The bis-triazole ligands often prefer an elongated octahedral geometry, with large M-N2 distances.

Experimental

General remarks. Reactions were carried out in ordinary glassware, and chemicals were used as purchased from commercial suppliers without further purification. The progress of all reactions was monitored by thin-layer chromatography (TLC) on silica gel 60F-254 plates (Merck, Darmstadt, Germany) and the spots were observed under UV light (254 nm). Purification of compounds using column chromatography was carried out on silica gel (0.063–0.2 mm) (Fluka, Buchs, Switzerland). The ^{1}H and ^{13}C NMR spectra were recorded in DMSO-d_6 or acetonitrile-d_3 at 298 K on a Bruker 300 or 600 MHz NMR spectrometer (Bruker Biospin, Rheinstetten, Germany). Chemical shifts were referenced to the signal of DMSO at δ: 2.50 ppm (^{1}H NMR) and δ: 39.50 ppm (^{13}C NMR) or acetonitrile at δ: 1.94 ppm (^{1}H NMR) and δ: 118.26 ppm (^{13}C NMR). The melting points of novel compounds were determined using a Kofler micro hot-stage (Reichert, Wien, Austria) apparatus. High-resolution mass spectra of the final compounds were recorded on a nanoAcquity Ultra Performance LC (Waters, Milford, MA, USA) and a Synapt G2-Si (Waters, Milford, MA, USA) using a UPLC column BEH130 C18 (100 µm × 100 mm, Waters, Milford, MA, USA). IR spectra were recorded using KBr pellets with a Bruker Alpha FT-IR spectrometer, in the 4000–350 cm^{-1} region. MS spectra were recorded on a high-performance liquid chromatography (HPLC)–MS system (Agilent Technologies 1200) coupled with a 6410 Triple-Quadrupole mass spectrometer, operating in a positive ESI mode. The UV–vis titrations were performed on a Cary 100 spectrophotometer. The CD spectra were recorded on a JASCO J-810 spectropolarimeter equipped with Peltier thermostat.

NMR measurements (*in situ*). Complexes were prepared by dissolving the ligand (0.5, 1 or 2 equiv) and metal salt (1 equiv) in approximately 0.6 mL CD_3CN. The NMR titration was performed by adding Zn(II) in the solution of the ligand to a solution of the ligand of the same concentration to avoid dilution.[53]

Synthesis of alkynes. *N*-(Prop-2-yn-1-yl)aniline (**2**), *N,N*-di(prop-2-yn-1-yl)aniline (**3**), *N*-(prop-2-yn-1-yl)benzothiazol-2-amine (**4**) and *N,N*-di(prop-2-yn-1-yl)benzothiazol-2-amine (**5**) were prepared according to known procedures.[35,36]

***N*-(Prop-2-yn-1-yl)-2,2′-dipyridylamine (1).** 2,2′-Dipyridylamine (500.0 mg, 2.92 mmol) was dissolved in anhydrous DMF (15 mL). Then NaH (101.4 mg, 4.23 mmol) was added, and the reaction mixture was stirred for 1.5 h at room temperature while bubbling with argon. Propargyl bromide (0.3 mL, 4.01 mmol) was added and the reaction was stirred for 24 h. The

reaction progress was monitored with TLC. The solvent was evaporated in a vacuum and the crude product purified using column chromatography (CH_2Cl_2 : CH_3OH = 100 : 1). Yield: 529.3 mg (2.53 mmol, 84%) of brown oil. ^{1}H NMR (300 MHz, DMSO-d_6) δ/ppm: 8.38 – 8.30 (2H, m, H-3, H-3'), 7.74 – 7.65 (2H, m, H-5, H-5'), 7.24 (2H, d, J = 8.4 Hz, H-6, H-6'), 7.05 – 6.97 (2H, m, H-4, H-4'), 4.93 (2H, d, J = 2.4 Hz, H-1''), 3.00 (1H, t, J = 2.4 Hz, H-3''). ^{13}C NMR (75 MHz, DMSO) δ/ppm: 156.08, 148.36, 138.18, 118.14, 114.79, 81.75, 73.55, 37.40.

Methyl-4-(prop-2-yn-1-ylamino)benzoate (**6**) and **methyl-4-(di(prop-2-ynyl)amino)benzoate** (**7**). Methyl-4-aminobenzoate (500.0 mg, 3.30 mmol) was dissolved in 10 mL of dry acetone and K_2CO_3 (2.43 g, 17.60 mmol) was added. The reaction mixture was refluxed for 1 h. Then KI (280.0 mg, 1.65 mmol) and propargyl bromide (0.4 mL, 6.60 mmol) were added and the reaction refluxed for 24 h. The reaction progress was monitored with TLC. The solvent was evaporated in a vacuum and the crude product purified using column chromatography (CH_2Cl_2). Yield: 67.0 mg (0.35 mmol, 11%) of yellow oil (**6**) and 323.0 mg (1.42 mmol, 43%) of white powder (**7**), m.p. = 72-76°C. ^{1}H NMR of **6** (300 MHz, DMSO-d_6) δ 7.78–7.67 (2H, m, H-3,5), 6.87 (1H, t, J = 5.9 Hz, NH), 6.74 – 6.60 (2H, m, H-2, 6), 3.98 – 3.90 (2H, m, H-1'), 3.75 (3H, s, H-8), 3.12 (1H, t, J = 2.4 Hz, H-3'). ^{13}C NMR of **6** (75 MHz, DMSO) δ 166.31, 151.85, 130.81, 116.83, 111.69, 81.32, 73.38, 51.30, 31.58. ^{1}H NMR of **7** (300 MHz, DMSO-d_6) δ 7.90–7.77 (2H, m, H-3,5), 7.00–6.86 (2H, m, H-2, 6), 4.27 (4H, s, H-1', H-1''), 3.79 (3H, s, H-8), 3.20 (2H, t, J = 2.3 Hz, H-3', H-3''). ^{13}C NMR of **7** (75 MHz, DMSO) δ 166.62 (C-7), 150.97 (C-1), 131.01 (C-3,5), 118.85 (C-4), 113.59 (C-2,6), 79.93 (C-2', C-2''), 75.57 (C-3', C-3''), 51.98 (C-8), 40.15 (C-1', C-1'').

General procedure for the synthesis of ligands 8a–11a. The alkyne (1 equiv) was dissolved in methanol and the azide (1.2 or 2.4 equiv) and copper(II) acetate (0.07 equiv) were added. The reaction mixture was stirred for 24 h at room temperature and the reaction progress was monitored with TLC. The solvent was evaporated in a vacuum and the crude product was purified using column chromatography.

***N*-[(1-Phenyl-1H-1,2,3-triazol-4-yl)methyl]-2,2'-dipyridylamine (8a).** Alkyne **1** (300.0 mg, 1.41 mmol), methanol 6 mL, azidobenzene (1.7 mL, 1.68 mmol), copper(II) acetate (18.0 mg, 0.10 mmol). Chromatography system, CH_2Cl_2 : CH_3OH (100 : 1). Yield: 228.4 mg (0.69 mmol, 49%) of white powder, m.p. = 116-118°C. ^{1}H NMR (300 MHz, DMSO-d_6) δ/ppm: 8.55 (1H, s, H-3''), 8.33 (2H, d, J = 3.7 Hz, H-3, H-3'), 7.84 (2H, d, J = 8.0 Hz, H-5'',9''), 7.73 – 7.62 (2H, m, H-6'',8''), 7.55 (2H, t, J = 7.6 Hz, H-5, H-5'), 7.45 (1H, t, J = 7.3 Hz, H-7''), 7.31 (2H, d, J = 8.4 Hz, H-6, H-6'), 7.03 – 6.94 (2H, m, H-4, H-4'), 5.50 (2H, s, H-1''). ^{13}C NMR (151 MHz, DMSO) δ/ppm: 156.63, 148.39, 146.76, 138.10, 137.04, 130.26, 128.95, 121.70, 120.39, 117.93, 115.08, 43.54. IR (KBr): *v/cm*$^{-1}$ 3444, 3139, 3074, 3052, 3011, 2987, 2939, 1582, 1560, 1501, 1470, 1429, 1382, 1344, 1320, 1244, 1175, 1045, 978, 876, 773, 758, 667, 605, 517, 408. MALDI-HRMS (m/z): calcd 329.1515 $[M+H]^+$, found 329.1530.

***N*-{[1-(4-Iodophenyl)-1H-1,2,3-triazol-4-yl]methyl}-2,2'-dipyridylamine (8b).** Alkyne **1** (38.0 mg, 0.18 mmol), methanol 8 mL, 1-azido-4-iodobenzene (0.43 mL, 0.22 mmol), copper(II) acetate (1.82 mg, 0.01 mmol). Chromatography system, CH_2Cl_2 : CH_3OH (200 : 1). Yield: 29.7 mg (0.06 mmol, 36%) of light brown powder, m.p. = 125-130°C. ^{1}H NMR (300 MHz, DMSO-d_6) δ/ppm: 8.59 (1H, s, H-3''), 8.39 – 8.26 (2H, m, H-3, H-3'), 7.95 – 7.83 (2H, m, H-7'', 9''), 7.79 – 7.62 (4H, m, H-4,6, H-4',6'), 7.30 (2H, d, J = 8.4 Hz, H-6'',10''), 6.98 (2H, s, H-5,5'), 5.49 (2H, s, H-1''). ^{13}C NMR (75 MHz, DMSO) δ/ppm: 156.08, 147.88, 146.48, 138.44, 137.60, 136.19, 121.79, 121.12, 117.45, 114.53, 94.02, 43.00. IR (KBr): *v/cm*$^{-1}$ 3433, 1673, 1583, 1470, 1425, 1040, 984, 821, 773, 606. MALDI-HRMS (m/z): calcd 455.0481 $[M+H]^+$, found 455.0497.

***N*-[1-(Benzyl-1H-1,2,3-triazol-4-yl)methyl]-2,2'-dipyridylamine (8c).** Alkyne **1** (78.2 mg, 0.37 mmol), methanol 3 mL, benzyl azide (0.90 mL, 0.45 mmol), copper(II) acetate (3.6 mg, 0.02 mmol). Chromatography system, CH_2Cl_2 : CH_3OH (200 : 1). Yield: 47.9 mg (0.14 mmol, 37%) of light-yellow powder, m.p. = 125-130°C. ^{1}H NMR (600 MHz, DMSO-d_6) δ/ppm: 8.31 – 8.27 (2H, m, H-3, H-3'), 7.91 (1H, s, H-3''), 7.68 – 7.62 (2H, m, H-5, H-5'), 7.35 – 7.27 (3H, m, H-7'',8'',9''), 7.25 (2H, d, J = 8.4 Hz, H-6'',10''), 7.19 – 7.15 (2H, m, H-6, H-6'), 6.96 (2H, dd, J = 6.9, 5.1 Hz, H-4, H-4'), 5.50 (2H, s, H-4''), 5.39 (2H, s, H-1''). ^{13}C NMR (75 MHz, DMSO) δ/ppm: 156.08, 147.81, 145.15, 137.57, 136.19, 128.62, 127.94, 127.63, 123.45, 117.38, 114.51, 52.49, 43.12. IR (KBr): *v/cm*$^{-1}$ 3442, 3111, 3065, 1584, 1558, 1470, 1425, 1379, 1283, 1228, 1211, 775, 735, 717, 604, 456. MALDI-HRMS (m/z): calcd 343.1671 $[M+H]^+$, found 343.1662.

***N*-{[1-((Phenylthio)methyl)-1H-1,2,3-triazol-4-yl]methyl}-2,2'-dipyridylamine (8d).** Alkyne **1** (100.0 mg, 0.47 mmol), methanol 2 mL, azidomethyl phenyl sulfide (0.08 mL, 0.56 mmol), copper(II) acetate (6.0 mg, 0.03 mmol). Chromatography system, CH_2Cl_2 : CH_3OH (200 : 1). Yield: 49.0 mg (0.13 mmol, 28%) of white powder, m.p. = 205-208°C. ^{1}H NMR (300 MHz, DMSO-d_6) δ/ppm: 8.29 – 8.27 (2H, m, H-3, H-3'), 7.70 – 7.60 (3H, m, H-7'',8'',9''), 7.29 – 7.15 (7H, m, H-4,5,6, H-4',5',6', H-3''), 7.00 – 6.93 (2H, m, H-6'',10''), 5.82 (2H, s, H-4''), 5.34 (2H, s, H-1''). ^{13}C NMR (151 MHz, DMSO) δ/ppm: 156.02, 147.82, 145.33, 137.57, 132.21, 130.96, 129.13, 127.77, 122.92, 117.40, 114.41, 51.71, 43.09. IR (KBr): *v/cm*$^{-1}$ 3442, 1584, 1561, 1471, 1438, 1380, 1228, 1042, 770, 754, 732, 601, 486. MALDI-HRMS (m/z): calcd 375.1392 $[M+H]^+$, found 375.1385.

***N,N*-Bis[(1-phenyl-1H-1,2,3-triazol-4-yl)methyl]aniline (9a).**[56] Alkyne **3** (100.0 mg, 0.60 mmol), methanol 2 mL, azidobenzene (2.8 mL, 1.42 mmol), copper(II) acetate (8.0 mg, 0.04 mmol). After 24 h at room temperature, the reaction was heated to 60°C for 24 h. Chromatography system, CH_2Cl_2 : CH_3OH (50 : 1). Yield: 48.9 mg (0.12 mmol, 20%) of white powder, m.p. = 202-205°C. ^{1}H NMR (300 MHz, DMSO-d_6) δ/ppm: 8.75 (2H, s, H-3',

H-3''), 7.93 – 7.82 (4H, m, H-5',9', H-5'',9''), 7.65 – 7.53 (4H, m, H-6',8', H-6'',8''), 7.53 – 7.42 (2H, m, H-7', H-7''), 7.22 – 7.10 (2H, m, H-3,5), 7.01 – 6.94 (2H, m, H-2,6), 6.65 (1H, t, *J* = 7.2 Hz, H-4), 4.81 (4H, s, H-1', H-1''). ^{13}C NMR (75 MHz, DMSO) *δ*/ppm: 148.25, 146.31, 137.10, 130.33, 129.44, 129.03, 121.78, 120.40, 117.19, 113.43, 46.16. IR (KBr): *ν/cm*$^{-1}$ 3442, 3124, 1600, 1507, 1374, 1225, 1042, 759, 745, 690, 508. MALDI-HRMS (m/z): calcd 408.1937 $[M+H]^+$, found 408.1929.

***N,N*-Bis{[1-(4-Iodophenyl)-1H-1,2,3-triazol-4-yl]methyl}aniline (9b).** Alkyne **3** (140.0 mg, 0.82 mmol), methanol 5 mL, 1-azido-4-iodobenzene (4.0 mL, 1.97 mmol), copper(II) acetate (7.3 mg, 0.04 mmol). After 24 h at room temperature, the reaction was transferred to a microwave reactor (1 h, 100°C, 300 W). Chromatography system, CH_2Cl_2 : CH_3OH (200 : 1). Yield: 42.8 mg (0.06 mmol, 8%) of white powder, m.p. > 250°C. ^{1}H NMR (300 MHz, DMSO-d_6) *δ*/ppm: 8.77 (2H s, H-3', H-3''), 7.94 (4H, d, *J* = 8.8 Hz, H6',8', H-6'',8''), 7.70 (4H, d, *J* = 8.8 Hz, H-5',9', H-5'',9''), 7.15 (2H, t, *J* = 8.0 Hz, H-3,5), 6.94 (2H, d, *J* = 8.1 Hz, H-2,6), 6.66 –6.62 (1H, m, H-4), 4.79 (4H, s, H-1', H-1''). ^{13}C NMR (151 MHz, DMSO) (δ/ppm): 147.75, 145.98, 138.52, 136.27, 128.94, 121.79, 121.19, 116.77, 112.97, 94.00, 45.65. IR (KBr): *ν/cm*$^{-1}$ 3443, 3121, 2925, 1600, 1495, 1374, 1224, 1041, 987, 820, 746, 691, 515. MALDI-HRMS (m/z): calcd 681.9689 $[M+Na]^+$, found 681.9681.

***N,N*-Bis[(1-benzyl-1H-1,2,3-triazol-4-yl)methyl]aniline (9c).**[56] Benzyl azide was prepared in situ: benzyl chloride (4.3 mL, 3.74 mmol) was dissolved in 6 mL of tert-butanol and 6 mL of water, followed by addition of sodium azide (182.7 mg, 2.81 mmol) and triethylamine (0.7 mL, 4.01 mmol). The reaction was stirred for 1 h at 60°C and the solvent evaporated in a vacuum. The prepared azide was dissolved in methanol and used in the click reaction according to the general procedure. The click reaction mixture was stirred at 60°C for 24 h.
Alkyne **3** (263.0 mg, 1.56 mmol), methanol 6 mL, copper(II) acetate (19.9 mg, 0.11 mmol). Chromatography system, CH_2Cl_2 : CH_3OH (50 : 1). Yield: 318.9 mg (0.73 mmol, 46%) of white powder, m.p. = 161-164°C. ^{1}H NMR (600 MHz, DMSO-d_6) *δ*/ppm: 8.01 (2H, s, H-3', H-3''), 7.37 – 7.29 (6H, m, H-7',8',9', H-7'',8'',9''), 7.28 – 7.21 (4H, m, H-6',10', H-6'',10''), 7.13 – 7.08 (2H, m, H-3,5), 6.85 (2H, d, *J* = 8.0 Hz, H-2,6), 6.61 (1H, t, *J* = 7.2 Hz, H-4), 5.53 (4H, s, H-4', H-4''), 4.61 (4H, s, H-1', H-1''). ^{13}C NMR (151 MHz, DMSO) *δ*/ppm: 147.65, 144.80, 136.11, 128.83, 128.67, 128.00, 127.73, 123.18, 116.46, 112.79, 52.63, 45.58. IR (KBr): *ν/cm*$^{-1}$ 3442, 3117, 3068, 1599, 1504, 1455, 1368, 1222, 1054, 750, 726, 709, 693, 462. MALDI-HRMS (m/z): calcd 436.2250 $[M+H]^+$, found 436.2249.

***N,N*-Bis{[1-(phenylthio)methyl)-1H-1,2,3-triazol-4-yl]methyl}aniline (9d).** Alkyne 3 (70.0 mg, 0.41 mmol), methanol 3 mL, azidomethyl phenyl sulfide (0.14 mL, 0.99 mmol), copper(II) acetate (3.6 mg, 0.02 mmol). After 24 h at room temperature, the reaction was transferred to a microwave reactor (1 h, 100°C, 300 W). Chromatography system, CH_2Cl_2 : CH_3OH (200 : 1). Yield: 79.9 mg (0.16 mmol, 39%) of light orange powder, m.p. = 106-110°C. ^{1}H NMR (300 MHz, DMSO) (δ/ppm): 7.85 (2H, s, H-3', H-3''), 7.39 – 7.24 (10H, m, H-6', H-7', H-8', H-9', H-10', H-6'', H-7'', H-8'', H-9'', H-10''), 7.13 (2H, t, J = 7.9 Hz, H-3, H-5), 6.81 (2H, d, J = 8.2 Hz, H-2, H-6), 6.65 (1H, t, J = 7.2 Hz, H-4), 5.86 (4H, s, H-4', H-4''), 4.54 (4H, s, H-1', H-1''). ^{13}C NMR (151 MHz, DMSO) (δ/ppm): 147.61, 132.27, 131.04, 129.18, 128.81, 127.81, 122.82, 116.69, 113.02, 51.91, 45.53. IR (KBr): *ν/cm*$^{-1}$ 3442, 3117, 1599, 1506, 1438, 1271, 1049, 746, 689, 491. MALDI-HRMS (m/z): calcd 499.1612 $[M+H]^+$, found 499.1620.

***N,N*-Bis[(1-phenyl-1H-1,2,3-triazol-4-yl)methyl]-2-aminobenzothiazole (10a).** Alkyne **5** (100.0 mg, 0.44 mmol), methanol 4 mL, azidobenzene (1.1 mL, 1.06 mmol), copper(II) acetate (5.8 mg, 0.03 mmol). After 24 h at room temperature, the reaction was heated to 60°C for 3 h. Chromatography system, pure CH_2Cl_2. Yield: 58.2 mg (0.12 mmol, 29%) of light yellow powder, m.p. = 185-188°C. Crystals suitable for X-ray diffraction were obtained by evaporation from methanol. ^{1}H NMR (300 MHz, DMSO-d_6) *δ*/ppm: 8.82 (2H, s, H-3', H-3''), 7.93 – 7.82 (4H, m, H-5',9', H-5'',9''), 7.78 (1H, d, *J* = 7.2 Hz, H-7), 7.62 – 7.44 (7H, m, H-4, H-6',7', 8', H-6'',7'',8''), 7.29 (1H, s, H-6), 7.09 (1H, s, H-5), 5.01 (4H, s, H-1', H-1''). ^{13}C NMR (75 MHz, DMSO) *δ*/ppm: 167.88, 152.83, 144.19, 137.02, 131.31, 130.30, 129.13, 126.39, 122.41, 121.75, 121.61, 120.52, 119.17, 45.93. IR (KBr): *ν/cm*$^{-1}$ 3441, 3139, 1598, 1563, 1531, 1502, 1444, 1358, 1292, 1230, 1051, 760, 748, 720, 690. MALDI-HRMS (m/z): calcd 465.1610 $[M+H]^+$, found 465.1605.

***N,N*-Bis{[1-(4-Iodophenyl)-1H-1,2,3-triazol-4-yl]methyl}-2-aminobenzothiazole (10b).** Alkyne **5** (100.0 mg, 0.44 mmol), methanol 3 mL, 1-azido-4-iodobenzene (2.1 mL, 1.06 mmol), copper(II) acetate (5.8 mg, 0.03 mmol). After 24 h at room temperature, the reaction was heated to 60°C for 24 h. Chromatography system, CH_2Cl_2 : CH_3OH (200 : 1). Yield: 262.2 mg (0.37 mmol, 84%) of light yellow powder, m.p. 262-265°C. ^{1}H NMR (300 MHz, DMSO-d_6) *δ*/ppm: 8.83 (2H, s, H-3', H-3''), 7.97 – 7.87 (4H, m, H-6',8', H-6'',8''), 7.78 (1H, d, *J* = 7.2 Hz, H-7), 7.72 – 7.65 (4H, m, H-5',9', H-5'',9''), 7.52 (1H, d, *J* = 7.5 Hz, H- 4), 7.33 – 7.26 (1H, m, H-6), 7.12 – 7.05 (1H, m, H-5), 4.99 (4H, s, H-1', H-1''). ^{13}C NMR (75 MHz, DMSO) *δ*/ppm: 167.84, 152.81, 144.38, 138.99, 136.64, 131.30, 126.40, 122.35, 121.77, 121.62, 119.18, 94.75, 45.92. IR (KBr): *ν/cm*$^{-1}$ 3444, 1531, 1495, 1454, 1356, 1236, 1048, 987, 816, 750, 507. MALDI-HRMS (m/z): calcd 716.9543 $[M+H]^+$, found 716.9530.

***N,N*-Bis[(1-benzyl-1H-1,2,3-triazol-4-yl)methyl]-2-aminobenzothiazole (10c).** Alkyne **5** (100.0 mg, 0.44 mmol), methanol 3 mL, benzyl azide (2.1 mL, 1.06 mmol), copper(II) acetate (5.4 mg, 0.03 mmol). Chromatography system, CH_2Cl_2 : CH_3OH (200 : 1). Yield: 119.2 mg (0.24 mmol, 55%) of white powder, m.p. = 150-154°C. Crystals suitable for X-ray diffraction were obtained by evaporation from acetonitrile. ^{1}H NMR (300 MHz, DMSO) (δ/ppm): 8.15 (2H, s, H-3', H-3''), 7.74 (1H, d, J = 0.7 Hz, H-7),7.47 (1H, d, J = 8.0 Hz, H-4), 7.42 – 7.36 (1H, m, H-5), 7.35 – 7.24 (10H, m, H-6', H-7', H-8', H-9', H-10' H-6', H-7'', H-8'', H-9'', H-10''),7.11 – 7.01 (1H, m, H-6), 5.56 (s, 4H, H-4', H-4''), 4.81 (4H, s, H-1', H-1''). ^{13}C NMR (75 MHz,

DMSO) (δ/ppm): 167.70, 152.81, 143.14, 136.49, 131.18, 129.19, 128.54, 128.31, 126.37, 124.32, 121.69, 121.56, 119.08, 53.22, 45.84. IR (KBr): *v/cm*$^{-1}$ 3444, 3119, 3065, 1598, 1565, 1546, 1454, 1438, 1383, 1308, 1205, 1124, 1054, 753, 724, 709. MALDI-HRMS (m/z): calcd 493.1923 $[M+H]^+$, found 493.1920. ESI-MS (m/z): 493.3 (M+H+, 100%)

***N,N*-Bis{[1-(phenylthio)methyl)-1H-1,2,3-triazol-4-yl]methyl} -2-aminobenzothiazole (10d).** Alkyne **5** (100.0 mg, 0.44 mmol), methanol 4 mL, azidomethyl phenyl sulfide (0.14 mL, 0.99 mmol), copper(II) acetate (5.5 mg, 0.03 mmol). After 24 h at room temperature, the reaction was heated to 60°C for 24 h. Chromatography system, CH_2Cl_2 : CH_3OH (200 : 1). Yield: 69.2 mg (0.12 mmol, 28%) of yellow oil. ^{1}H NMR (600 MHz, DMSO-d_6) *δ*/ppm: 7.97 (2H, s, H-3', H-3''), 7.80 – 7.75 (1H, m, H-7), 7.48 (1H, d, *J* = 7.8 Hz, H-4), 7.38 – 7.34 (4H, m, H-6',10', H-6'',10''), 7.33 – 7.27 (2H, m, H-5,6), 7.27 – 7.20 (6H, m, H-7',8',9', H-7'',8'',9''), 5.90 (4H, s, H-4', H-4''), 4.71 (4H, s, H-1', H-1''). ^{13}C NMR (151 MHz, DMSO) *δ*/ppm: 167.04, 152.23, 142.66, 132.17, 130.96, 130.71, 129.17, 127.76, 125.89, 123.51, 121.27, 121.09, 118.64, 51.81, 45.18. IR (KBr): *v/cm*$^{-1}$ 3442, 1537, 1439, 1380, 1283, 1225, 1201, 1046, 748, 725, 689, 489. MALDI-HRMS (m/z): calcd 557.1364 $[M+H]^+$, found 557.1386.

Methyl-4-{bis[(1-phenyl-1H-1,2,3-triazole-4-yl)methyl]amino}benzoate (**11a**). Alkyne **7** (200.0 mg, 0.88 mmol), methanol 10 mL, azidobenzene (4.2 mL, 2.11 mmol), copper(II) acetate (11.2 mg, 0.06 mmol). Stirred for 24 h at 60°C. Chromatography system, CH_2Cl_2 : CH_3OH (100 : 1). Yield: 246.3 mg (0.53 mmol, 60%) of light yellow powder, m.p. = 180-185°C. ^{1}H NMR (600 MHz, DMSO-d_6) δ 8.78 (2H, s, H-3', H-3''), 7.90–7.82 (4H, m, H-5',9', H-5'',9''), 7.80–7.74 (2H, m, H-3, 5), 7.61–7.54 (4H, m, H-6', 8', H-6'', 8''), 7.51–7.44 (2H, m, H-7', 7''), 7.07–7.02 (2H, m, H-2, 6), 4.90 (4H, s, H-1', 1''), 3.74 (3H, s, H-8). ^{13}C NMR (151 MHz, DMSO) δ 166.16 (C-7), 151.29 (C-1), 144.97 (C-2', C-2''), 136.56 (C-4', C-4''), 130.77 (C-3,5), 129.83 (C-6',8', C-6'',8''), 128.60 (C-7', C-7''), 121.44 (C-3', C-3''), 119.96 (C-5',9', C-5'',9''), 116.94 (C-4), 111.80 (C-2,6), 51.32 (C-8), 45.37 (C-1', C-1''). IR (KBr): *v/cm*$^{-1}$ 3441, 3129, 3088, 2949, 1702, 1606, 1521, 1501, 1287, 1196, 1112, 1049, 827, 762, 689, 516. MALDI-HRMS (m/z): calcd 466,1991 $[M+H]^+$, found 466,1968.

4-{Bis[(1-phenyl-1H-1,2,3-triazole-4-yl)methyl]amino}benzoic acid (**12a**).[38] **11a** (150.6 mg, 0.32 mmol) was dissolved in 20 mL of CH_2Cl_2/CH_3OH (9:1) and a methanolic solution of NaOH (1 M, 5.0 mL) was added. The reaction was stirred at 60°C for 24 h. The reaction progress was monitored with TLC and a methanolic solution of NaOH (1 M, 10.0 mL) was added in small portions. The solvent was evaporated in a vacuum, the crude product dissolved in water and washed with diethyl-ether. The aqueous layer was cooled, acidified to pH = 2 with HCl (5 M) and extracted with CH_2Cl_2. The organic layer was evaporated in a vacuum. No further purification was performed. Yield: 132.5 mg (0.29 mmol, 91%), white powder. ^{1}H NMR (300 MHz, DMSO-d_6) δ 12.14 (1H, s, H-8), 8.79 (2H, s, H-3', H-3''), 7.92 – 7.83 (4H, m, H- H-5',9', H-5'', 9''), 7.75 (2H, d, *J* = 8.9 Hz, H-3, 5), 7.63–7.53 (4H, m, H-6',8', H-6'',8''), 7.53–7.43 (2H, m, H-7', 7''), 7.02 (2H, d, *J* = 9.1 Hz, H-2, 6), 4.90 (4H, s, H-1', 1''). ^{13}C NMR (151 MHz, Acetonitrile-d_3) δ 152.66 (C-7), 146.34 (C-1), 132.31 (C-2', C-2''), 130.74 (C-4', 4''), 129.64 (C-3, 6', 6'', 7', 7'', 8'', 8''), 122.13 (C-5', 5'', 9', 9''), 121.33 (C-3', 3''), 113.03 (C-2, 6), 46.92 (C-1', C-1''). IR (KBr): *v/cm*$^{-1}$ 3451, 3130, 3073, 1072, 1677, 1601, 1524, 1502, 1289, 1245, 1192, 1050, 932, 831, 761, 690, 516. MALDI-HRMS (m/z): calcd 452.1835 $[M+H]^+$, found 452.1822.

Methyl-(*S*)-3-{4-[bis((1-phenyl-1H-1,2,3-triazol-4-yl)methyl)amino]benzamido}-4-phenylbutanoate (**13a**). **12a** (120.4 mg, 0.27 mmol) was dissolved in acetonitrile (20.0 mL) and TBTU (86.7 mg, 0.27 mmol), HOBt (36.5 mg, 0.27 mmol) and DIPEA (0.18 mL, 1.07 mmol) were added. The reaction was mixed for 1 h at room temperature, followed by addition of L-phenylalanine methyl ester hydrochloride (58.2 mg, 0.27 mmol). The reaction mixture was stirred for 2 days, the solvent evaporated in a vacuum, the crude product dissolved in CH_2Cl_2 and washed with saturated $NaHCO_3$ and water. The organic layer was dried over anhydrous $NaHCO_3$, filtered and evaporated in a vacuum. The crude product was purified using automated flash chromatography (0-5% CH_3OH in CH_2Cl_2). Yield: 80.2 mg (0.13 mmol, 49%) of white powder. ^{1}H NMR (600 MHz, $CDCl_3$) (δ/ppm): 7.86 (2H, s, H-3', H-3''), 7.70 – 7.62 (5H, m, H-Ph), 7.50 – 7.46 (4H, m, H-Ph), 7.44 – 7.38 (2H, m, H-Ph), 7.30 – 7.21 (4H, m, H-Ph), 7.14 – 7.10 (2H, m, H-Ph), 6.98 – 6.94 (2H, m, H-Ph), 6.41 (1H, d, J = 7.6 Hz, H-8), 5.11 – 5.00 (1H, m, H-9), 4.88 (4H, s, H-1', H-1''), 3.73 (3H, s, H-18), 3.28 – 3.16 (2H, m, H-10). ^{13}C NMR (151 MHz, $CDCl_3$) (δ/ppm): 172.41, 166.59, 150.42, 145.50, 137.01, 136.15, 129.88, 129.46, 129.02, 128.98, 128.74, 127.26, 122.74, 120.66, 120.40, 112.52, 53.49, 52.45, 46.86, 38.75, 38.18. IR (KBr): *v/cm*$^{-1}$ 3424, 3349, 3135, 2947, 1738, 1634, 1608, 1503, 1342, 1227, 1203, 1044, 832, 759, 700, 689, 515. MALDI-HRMS (m/z): calcd 613.2676 $[M+H]^+$, found 613.2692.

Preparation of single crystals, General procedure. Saturated methanol or dichloromethane solutions of the ligand (2 equiv) and methanol solution of the metal salt (1 equiv) were heated and boiled shortly in separate beakers until completely dissolved. The metal salt solution was added to the ligand solution and the mixture was cooled to room temperature and left partially covered for slow evaporation or in a tank filled with diethyl-ether until crystallization occurred. The solvent was decanted and the crystals washed with diethyl ether and air-dried. The yields of obtained complexes were low, due to the necessity of SiF_6^{2-} formation from the glass reaction vessel and due to multiple species being in equilibrium as observed in UV-Vis and NMR measurements.

$[Cu(8a)_2](BF_4)_2$, $8a_{Cu}$. 8a (14.0 mg, 0.04 mmol), $Cu(BF_4)_2$ x nH_2O (5.1 mg, 0.02 mmol). A small amount of light-blue cubic crystals suitable for X-ray diffraction were obtained by diffusion of diethyl-ether. IR (KBr): *v/cm*$^{-1}$ 3441, 3149, 2967, 1601, 1468, 1448, 1363, 1271, 1066, 802, 762, 693, 609, 545, 520, 437.

[Cu(8d)$_2$(H$_2$O)$_2$](SiF$_6$) x 2CH$_3$OH, 8d$_{Cu}$. 8d (7.2 mg, 0.02 mmol), Cu(BF$_4$)$_2$ x nH$_2$O (2.3 mg, 0.01 mmol). Yield: 1.9 mg (0.002 mmol, 19%) of purple rhombic crystals suitable for X-ray diffraction. IR (KBr): *ν/cm^{-1}* 3443, 1631, 1604, 1468, 1446, 1083, 1051, 795, 744, 693.

[Cu(9c)$_2$](SiF$_6$), 9c$_{Cu}$. 9c (15.7 mg, 0.04 mmol), Cu(BF$_4$)$_2$ x nH$_2$O (4.3 mg, 0.02 mmol). Yield: 5.2 mg (0.005 mmol, 27%) of brown cubic crystals suitable for X-ray diffraction. IR (KBr): *ν/cm^{-1}* 3444, 3149, 1600, 1499, 1457, 1214, 1064, 766, 752, 724, 702, 521.

[Cu(10c)$_2$](SiF$_6$), 10c$_{Cu}$. 10c (15.3 mg, 0.03 mmol), Cu(BF$_4$)$_2$ x nH$_2$O (3.7 mg, 0.02 mmol). Yield: A small amount of pink cubic crystals suitable for X-ray diffraction were obtained by slow evaporation of the solvent. IR (KBr): *ν/cm^{-1}* 3444, 3135, 3090, 1630, 1531, 1448, 866, 760, 728, 477.

Calculations

All molecular geometries were optimized using a very efficient DFT M05-2X/6–31+G(d)/LanL2DZ + ECP model, known to be successful in reproducing geometries, dipole moments, and hemolytic bond energies in various metal complexes,[57,58] and in accordance with our comparative analysis with other DFT approaches on similar systems.[21] To account for the effect of the acetonitrile solution, during geometry optimization, we included the implicit SMD solvation model (ε = 35.688), being in line with our earlier results.[17,18,21] Thermal corrections were extracted from the corresponding frequency calculations, and all of the presented results correspond to differences in the Gibbs free energies. All calculations were performed using the Gaussian 16 software.[59] Cartesian coordinates for all computed molecules are collected in a single text file readable by the Mercury program (version 3.3 or later).[60]

X-Ray Crystallography. The X-ray intensity data were collected on an Oxford Diffraction Xcalibur CCD diffractometer using monochromatic Cu Kα (λ = 1.54184 Å) radiation. For temperature conditions, see Table S1. The data were processed with the CrysalisPro program[61] (unit cell determination and data reduction). The crystals of **8d$_{Cu}$** showed bad diffraction properties, only several intensities at ϑ angles higher than 35° were unreliably determined, therefore reflections only with ϑ < 35° were used in structural determination. The structures were solved by direct methods with the SHELXT program[62] and refined against F^2 on all data by a full-matrix least-squares procedure with the SHELXL program.[63] Due to the low number of reliably determined reflections for **8d$_{Cu}$**, all atoms in this structure (except Cu, Si and F) were refined with isotropic displacement parameters, for all other structures non-hydrogen atoms were refined with anisotropic displacement parameters. All H atoms were included at geometrically calculated positions, H atoms from coordinated water molecule in **8d$_{Cu}$**, were additionally restraint to typical O-H bonds of 0.82 Å and distances toward nearest acceptor atoms. Solvent-accessible voids of volume 252 and 241 Å^3 were found in structures **8d$_{Cu}$** and **10c$_{Cu}$**, respectively. (In **10c$_{Cu}$** there are two symmetry related voids of volume 241 Å^3 in the unit cell.) Electron densities from these voids were treated by SQUEEZE procedure in the PLATON program[64], in combination with the SHELXL refinements.[63,64] Disorder of some molecular groups was detected in the structures **10c** and **9c$_{Cu}$**. Two orientations of such groups were modelled and occupancies of different orientations were refined: in **10c** the benzothiazole group was disordered, in **9c$_{Cu}$** phenyl ring from the benzyl group attached to triazole was found to occupy two orientations. To some extent, the benzothiazole group in **10a** can also be considered as disordered, due to very elongated displacement parameters for atoms in this group. For atoms in these disordered groups, the additional distance restraints were used in refinement (**10a**) or positions of atoms were fitted to regular hexagon with C-C distance of 1.39 Å (**9c$_{Cu}$**) with the additional rigid body restraints for anisotropic displacement parameters (DELU and SIMU). The BF_4^- anion in the structure of **8a$_{Cu}$** was also found to be disordered over two positions and orientations. The anion was treated as a rigid body of ideal tetrahedral symmetry with a B–F bond length of 1.36 Å with additional rigid body restraints for anisotropic displacement parameters (DELU), as recommended for refinements of disordered BF_4^- contentions.[65] All details for X-ray diffraction studies in this publication are collected in Table S1. CCDC 1993924-1993929 contain the supplementary crystallographic data for this paper. These data can be obtained free of charge via www.ccdc.cam.ac.uk/data_request/cif, or by emailing data_request@ccdc.cam.ac.uk, or by contacting The Cambridge Crystallographic Data Centre, 12 Union Road, Cambridge CB2 1EZ, UK; fax: +44 1223 336033.

Conflicts of interest

There are no conflicts to declare.

Corresponding Author

*E-mail:
Srecko.Kirin@irb.hr
sraic@fkit.hr
Robert.Vianello@irb.hr

ORCID

Natalija Pantalon Juraj: 0000-0002-0357-5817
Marko Krklec: 0000-0003-3862-6415
Tiana Novosel: 0000-0003-4687-3723
Berislav Perić: 0000-0002-2397-2836
Robert Vianello: 0000-0003-1779-4524
Silvana Raić-Malić: 0000-0001-5021-8970
Srećko I. Kirin: 0000-0002-0500-2422

Acknowledgements

We greatly appreciate the financial support of the Croatian Science Foundation (grant numbers IP–2013–11–5596 and IP-2014-09-1461)

References

1 Q. V. C. van Hilst, N. R. Lagesse, D. Preston and J. D. Crowley, *Dalton Trans.*, 2018, **47**, 997–1002.

2 D. Wang, D. Denux, J. Ruiz and D. Astruc, *Adv. Synth. Catal.*, 2013, **355**, 129–142.

3 J. T. Simmons, J. R. Allen, D. R. Morris, R. J. Clark, C. W. Levenson, M. W. Davidson and L. Zhu, *Inorg. Chem.*, 2013, **52**, 5838–5850.

4 T. L. Mindt, H. Struthers, L. Brans, T. Anguelov, C. Schweinsberg, V. Maes, D. Tourwe and R. Schibli, *J. Am. Chem. Soc.*, 2006, **128**, 15096–15097.

5 J. P. Byrne, J. A. Kitchen and T. Gunnlaugsson, *Chem. Soc. Rev.*, 2014, **43**, 5302–5325.

6 B. Štefane, F. Perdih, A. Višnjevac and F. Požgan, *New J. Chem.*, 2015, **39**, 566–575.

7 S. Anjana, S. Donring, P. Sanjib, B. Varghese and N. N. Murthy, *Dalton Trans.*, 2017, **46**, 10830–10836.

8 B. J. Pages, J. Sakoff, J. Gilbert, Y. Zhang, F. Li, D. Preston, J. D. Crowley and J. R. Aldrich-Wright, *J. Inorg. Biochem.*, 2016, **165**, 92–99.

9 S. V Kumar, S. O. Scottwell, E. Waugh, C. J. McAdam, L. R. Hanton, H. J. L. Brooks and J. D. Crowley, *Inorg. Chem.*, 2016, **55**, 9767–9777.

10 A. Sinopoli, F. A. Black, C. J. Wood, E. A. Gibson and P. I. P. Elliott, *Dalton Trans.*, 2017, **46**, 1520–1530.

11 M. Gaber, H. A. El-Ghamry, S. K. Fathalla and M. A. Mansour, *Mater. Sci. Eng. C. Mater. Biol. Appl.*, 2018, **83**, 78–89.

12 H. Struthers, T. L. Mindt and R. Schibli, *Dalton Trans.*, 2010, **39**, 675–696.

13 R. A. Murcia, S. M. Leal, M. V Roa, E. Nagles, A. Munoz-Castro and J. J. Hurtado, *Molecules*, 2018, **23**, E2013.

14 Y. Bourne, H. C. Kolb, Z. Radić, K. B. Sharpless, P. Taylor and P. Marchot, *Proc. Natl. Acad. Sci. U. S. A.*, 2004, **101**, 1449–1454.

15 D. Huang, P. Zhao and D. Astruc, *Coord. Chem. Rev.*, 2014, **272**, 145–165.

16 B. Schulze and U. S. Schubert, *Chem. Soc. Rev.*, 2014, **43**, 2522–2571.

17 Đ. Škalamera, E. Sanders, R. Vianello, A. Maršavelski, A. Pevec, I. Turel and S. I. Kirin, *Dalton Trans.*, 2016, **45**, 2845–2858.

18 N. Pantalon Juraj, G. Miletić, B. Perić, Z. Popović, N. Smrečki, R. Vianello and S. I. Kirin, *Inorg. Chem.*, 2019, **58**, 16445–16457.

19 N. Smrečki, O. Jović, K. Molčanov, B.-M. Kukovec, I. Kekez, D. Matković-Čalogović and Z. Popović, *Polyhedron*, 2017, **130**, 115–126.

20 N. Smrečki, V. Stilinovic, O. Jovic, B. Kukovec and Z. Popovic, *Inorg. Chim. Acta*, 2017, **462**, 57–63.

21 N. Pantalon Juraj, S. Muratović, B. Perić, N. Šijaković Vujičić, R. Vianello, D. Žilić, Z. Jagličić and S. I. Kirin, *Cryst. Growth Des.*, 2020, **20**, 2440–2453.

22 B. Maity, S. Gadadhar, T. K. Goswami, A. A. Karande and A. R. Chakravarty, *Dalton Trans.*, 2011, **40**, 11904–11913.

23 D. Schweinfurth, J. Krzystek, I. Schapiro, S. Demeshko, J. Klein, J. Telser, A. Ozarowski, C.-Y. Su, F. Meyer, M. Atanasov, F. Neese and B. Sarkar, *Inorg. Chem.*, 2013, **52**, 6880–6892.

24 D. Schweinfurth, S. Demeshko, S. Hohloch, M. Steinmetz, J. G. Brandenburg, S. Dechert, F. Meyer, S. Grimme and B. Sarkar, *Inorg. Chem.*, 2014, **53**, 8203–8212.

25 D. Schweinfurth, S. Demeshko, M. M. Khusniyarov, S. Dechert, V. Gurram, M. R. Buchmeiser, F. Meyer and B. Sarkar, *Inorg. Chem.*, 2012, **51**, 7592–7597.

26 D. Schweinfurth, J. Krzystek, M. Atanasov, J. Klein, S. Hohloch, J. Telser, S. Demeshko, F. Meyer, F. Neese and B. Sarkar, *Inorg. Chem.*, 2017, **56**, 5253–5265.

27 X. You and Z. Wei, *Transit. Met. Chem.*, 2014, **39**, 675–680.

28 A. K. Mondal, J. Jover, E. Ruiz and S. Konar, *Chem. – A Eur. J.*, 2017, **23**, 12550–12558.

29 M. G. Sommer, Y. Rechkemmer, L. Suntrup, S. Hohloch, M. van der Meer, J. van Slageren and B. Sarkar, *Dalton Trans.*, 2016, **45**, 17770–17781.

30 D. Schweinfurth, M. G. Sommer, M. Atanasov, S. Demeshko, S. Hohloch, F. Meyer, F. Neese and B. Sarkar, *J. Am. Chem. Soc.*, 2015, **137**, 1993–2005.

31 T. Benko, Master Thesis, Faculty of Chemical Engineering and Technology, University of Zagreb, 2018.

32 M. Krklec, Master Thesis, Faculty of Chemical Engineering and Technology, University of Zagreb, 2019.

33 G.-C. Kuang, P. M. Guha, W. S. Brotherton, J. T. Simmons, L. A. Stankee, B. T. Nguyen, R. J. Clark and L. Zhu, *J. Am. Chem. Soc.*, 2011, **133**, 13984–14001.

34 W. S. Brotherton, H. A. Michaels, J. T. Simmons, R. J. Clark, N. S. Dalal and L. Zhu, *Org. Lett.*, 2009, **11**, 4954–4957.

35 D. Yim, H. Yoon, C.-H. Lee and W.-D. Jang, *Chem. Commun.*, 2014, **50**, 12352–12355.

36 M. K. Singh, R. Tilak, G. Nath, S. K. Awasthi and A. Agarwal, *Eur. J. Med. Chem.*, 2013, **63**, 635–644.

37 J.-C. Castillo, J. Orrego-Hernández and J. Portilla, *Eur. J. Org. Chem.*, 2016, **2016**, 3824–3835.

38 V. Theodorou, K. Skobridis, A. G. Tzakos and V. Ragoussis, *Tetrahedron Lett.*, 2007, **48**, 8230–8233.

39 R. Diaz-Torres and S. Alvarez, *Dalton Trans.*, 2011, **40**, 10742–10750.

40 H. Casellas, A. Pevec, B. Kozlevčar, P. Gamez and J. Reedijk, *Polyhedron*, 2005, **24**, 1549–1554.

41 K. Saihara, Y. Yoshimura, H. Fujimoto and A. Shimizu, *J. Mol. Liq.*, 2016, **219**, 493–496.

42 R. G. Pearson, *J. Am. Chem. Soc.*, 1963, **85**, 3533–3539.

43 R. G. Pearson, *Coord. Chem. Rev.*, 1990, **100**, 403–425.

44 C. Andreini, G. Cavallaro and S. Lorenzini, *Bioinformatics*, 2012, **28**, 1658–1660.

45 S. P. Foxon, O. Walter and S. Schindler, *Eur. J. Inorg. Chem.*, 2002, **2002**, 111–121.

46 S. I. Kirin, H. P. Yennawar and M. E. Williams, *Eur. J. Inorg. Chem.*, 2007, **2007**, 3686–3694.

47 K. I. Alexopoulou, M. Leibold, O. Walter, T. A. Zevaco and S. Schindler, *Eur. J. Inorg. Chem.*, 2017, **2017**, 4722–4732.

48 M. A. Halcrow, *Chem. Soc. Rev.*, 2013, **42**, 1784–1795.

49 P. S. Donnelly, S. D. Zanatta, S. C. Zammit, J. M. White and S. J. Williams, *Chem. Commun.*, 2008, 2459–2461.

50 J. Geng, J. Lindqvist, G. Mantovani, G. Chen, C. T. Sayers, G. J. Clarkson and D. M. Haddleton, *QSAR Comb. Sci.*, 2007, **26**, 1220–1228.

51 M. G. Sommer, R. Marx, D. Schweinfurth, Y. Rechkemmer, P. Neugebauer, M. van der Meer, S. Hohloch, S. Demeshko, F. Meyer, J. van Slageren and B. Sarkar, *Inorg. Chem.*, 2017, **56**, 402–413.

52 A. D. Bain and G. J. Duns, in *Analytical Spectroscopy Library*, 1997, pp. 227–263.

53 P. Thordarson, *Chem. Soc. Rev.*, 2011, **40**, 1305–1323.

54 P. Gans, A. Sabatini and A. Vacca, *Talanta*, 1996, **43**, 1739–1753.

55 S. I. Kirin, H.-B. Kraatz and N. Metzler-Nolte, *Chem. Soc. Rev.*, 2006, **35**, 348–354.

56 Z.-J. He, M.-H. Wei, X.-L. Zhang, J.-M. Chen and S.-R. Sheng, *Synth. Commun.*, 2019, **49**, 2760–2766.

57 E. A. Amin and D. G. Truhlar, *J. Chem. Theory Comput.*, 2008, **4**, 75–85.

58 C. J. Cramer and D. G. Truhlar, *Phys. Chem. Chem. Phys.*, 2009, **11**, 10757–10816.

59 *Gaussian 16, Revision C.01, M. J. Frisch, G. W. Trucks, H. B.*

Schlegel, G. E. Scuseria, M. A. Robb, J. R. Cheeseman, G. Scalmani, V. Barone, G. A. Petersson, H. Nakatsuji, X. Li, M. Caricato, A. V. Marenich, J. Bloino, B. G. Janesko, R. Gomperts, B. Mennucci, H. P. Hratchian, J. V. Ortiz, A. F. Izmaylov, J. L. Sonnenberg, D. Williams-Young, F. Ding, F. Lipparini, F. Egidi, J. Goings, B. Peng, A. Petrone, T. Henderson, D. Ranasinghe, V. G. Zakrzewski, J. Gao, N. Rega, G. Zheng, W. Liang, M. Hada, M. Ehara, K. Toyota, R. Fukuda, J. Hasegawa, M. Ishida, T. Nakajima, Y. Honda, O. Kitao, H. Nakai, T. Vreven, K. Throssell, J. A. Montgomery, Jr., J. E. Peralta, F. Ogliaro, M. J. Bearpark, J. J. Heyd, E. N. Brothers, K. N. Kudin, V. N. Staroverov, T. A. Keith, R. Kobayashi, J. Normand, K. Raghavachari, A. P. Rendell, J. C. Burant, S. S. Iyengar, J. Tomasi, M. Cossi, J. M. Millam, M. Klene, C. Adamo, R. Cammi, J. W. Ochterski, R. L. Martin, K. Morokuma, O. Farkas, J. B. Foresman, and D. J. Fox, Gaussian, Inc., Wallingford CT, 2016.

60 *The program Mercury is available at no cost from www.ccdc.cam.ac.uk/products/mercury*

61 CrysAlisPro version 1.171.39.46; Rigaku OD, 2018.

62 G. M. Sheldrick, *Acta Cryst.*, 2015, **A71**, 3–8.

63 G. M. Sheldrick, *Acta Cryst.*, 2015, **C71**, 3–8.

64 A. L. Spek, *Acta Cryst.*, 2015, **C71**, 9–18.

65 J. J. Allen and A. R. Barron, *https//cnx.org/exports/6499f6de-92bb-4b4e-97f9-eac6fb9581cb@3.pdf/refinement-of-crystallographicdisorder-in-the-tetrafluoroborate-anion-3.pdf (from Raja, P. M. V.; Barron, A. R. Phys. Methods Chem. Nano Sci. Rice Univ. 2019).*

Graphical Abstract

Click chemistry is a simple way of preparing a wide scope of ligands that can coordinate metals such as Cu(II) and Zn(II), forming complexes of different stoichiometry, geometry and stereochemistry.